

1                                   **Infection of endotheliotropic human**  
2                                   **cytomegalovirus of trabecular meshwork cells**

3   Running title: CMV infection of trabecular meshwork cells

4   Daisuke Shimizu<sup>1,4</sup>, Dai Miyazaki<sup>1</sup>, Yumiko Shimizu<sup>1</sup>, Mayumi Hosogai<sup>2</sup>, Isao

5   Kosugi<sup>3</sup>, Yoshitsugu Inoue<sup>1</sup>

6   <sup>1</sup>Ophthalmology and Visual Science, Tottori University Faculty of Medicine, Yonago

7   City, Japan.

8   <sup>2</sup>Department of Ophthalmology, Gunma University Graduate School of Medicine,

9   Maebashi City, Japan

10  <sup>3</sup>Regenerative and Infectious Pathology, Hamamatsu University, School of Medicine

11  <sup>4</sup>Department of Ophthalmology, Chiba University Graduate School of Medicine,

12  Chiba City, Japan

13  
14  Correspondence to Dai Miyazaki, MD

15  36-1 Nishicho, Yonago 683-8504, Japan

16  tel:81-859-38-6617   fax:81-859-38-6619

17  miyazaki-ttr@umin.ac.jp

18  26 references and 9 figures

19  **Keywords:** cytomegalovirus; corneal endothelial cells; trabecular meshwork;

20 secondary glaucoma; endotheliitis

21 **Abstract**

22 **Purpose:** Human cytomegalovirus (HCMV) infections can cause endotheliitis which  
23 is associated with an elevation of the intraocular pressure (IOP). However, the  
24 mechanism of the IOP elevation has not been determined. The purpose of this study  
25 was to determine whether HCMV strains which are capable of infecting corneal  
26 endothelial cells can also replicate, induce anti-viral responses, and can reorganize  
27 the actin cytoskeleton in trabecular meshwork cells.

28 **Study design:** Experimental study design

29 **Methods:** Cultured primary human trabecular meshwork cells (HTMCs) were  
30 infected with the Towne or TB40/E strains of HCMV. TB40/E is trophic for vascular  
31 endothelial and corneal endothelial cells. Real-time PCR, western blot, and  
32 fluorescent immunostaining have been used to determine whether HCMV-infected  
33 HTMCs will support the expression of viral mRNA and protein, allow viral replication,  
34 and elicit anti-viral host responses. We also determined whether lytic replication was  
35 present after an HCMV infection.

36 **Results:** HCMV infection led to the expression of viral mRNA and proteins of IE1,  
37 glycoprotein B(gB), and pp65. TB40/E infection induced interferon- $\beta$ , a sign of host  
38 anti-viral immune response and MCP-1. Together with the induction of the regulators  
39 of actin cytoskeleton, myosin phosphatase Rho interacting protein (MPRIP) and

40 monocyte chemotactic protein-1 (MCP-1), TB40/E induced a high level of expression  
41 of viral proteins, including IE1, gB, and pp65 as well as actin stress fiber formation,  
42 and achieved pathogenically high viral titers.

43 **Conclusions:** Human trabecular meshwork cells support the replication of  
44 endotheliotropic TB40/E strain of HCMV which indicates that this strain may have  
45 high virulence for trabecular meshwork.

46 **Introduction**

47 Human cytomegalovirus (HCMV) infection can lead to endotheliitis which is  
48 associated with an elevation of the intraocular pressure (IOP) and endothelial cell  
49 loss [1]. Its chronic and relapsing nature resembles the clinical characteristic of  
50 Fuchs iridocyclitis and Posner-Schlossman syndrome. These disease entities are  
51 characterized by chronic and relapsing elevations of the IOP, and HCMV infection  
52 has been recognized to be an important causative pathogen for these relapses and  
53 elevations.

54

55 In HCMV endotheliitis, the IOP elevation and endothelial inflammation frequently  
56 recurs during the long course of the disease process. The IOP elevation can last for  
57 months or years, and the eye can become refractory to the IOP lowering  
58 medications. Because of this, these patients often require filtering surgery. The  
59 findings strongly suggest that the HCMV may actively proliferate in the trabecular  
60 meshwork and corneal endothelial cells.

61

62 The IOP elevation during the long disease course of HCMV endotheliitis will damage  
63 the trabecular meshwork cells which can then lead to a severe reduction of aqueous  
64 outflow. However, there is no definitive proof that surgically-obtained trabecular

65 meshwork tissue was permissive for HCMV infection. Because filtering surgery is  
66 generally performed after years of IOP elevation, the trabecular meshwork cells were  
67 already damaged. This may explain the absence of HCMV proteins in the trabecular  
68 meshwork specimens.

69

70 When HCMV infects permissive cells, latent infection can be established. During the  
71 latency phase, detection of viral protein antigen is very difficult unless the specimen  
72 is collected during the reactivation phase. We have shown that corneal endothelial  
73 cells can be infected by the Towne strain, the TB40/E strain, and a clinically-isolated  
74 strain of HCMV [2, 3]. However, the efficiency of infection measured by TCID<sub>50</sub> is  
75 markedly different depending on the strain, and vascular endotheliotropic TB40/E  
76 was also tropic for corneal endothelium. We have hypothesized that endotheliotropic  
77 HCMV strain will infect trabecular meshwork cells more efficiently than non-tropic  
78 strains of HCMV.

79

80 Thus, the purpose of this study was to determine whether endotheliotropic strain of  
81 HCMV can infect trabecular meshwork cells and reorganize the actin stress fibers. In  
82 addition, we examined whether HCMV infection will induce strong immune  
83 responses which may explain the increased outflow resistance of the trabecular

84 meshwork in eyes with HCMV infection.

85

## 86 **Materials and Methods**

87 All protocols and methods adhered to the tenets of the Declaration of Helsinki, and  
88 the study was approved by the Ethics Committee of Tottori University.

89

### 90 **Cells and virus**

91 Human trabecular meshwork cells (HTMC) were isolated from trabecular tissues  
92 stripped from cadaver eyes donated for research purposes. (ScienCell, Carlsbad,  
93 CA) The HTMCs were propagated to confluence on 6- or 96-well plates in  
94 Dulbecco's modified Eagle's medium (DMEM; Gibco, Grand Island, NY)  
95 supplemented with 15% fetal bovine serum.

96

97 A standard laboratory strain, Towne, and an endotheliotropic HCMV strain, TB40/E,  
98 were used. The Towne strain is a representative laboratory strain together with  
99 AD169, and is one of most widely used HCMV strain. The Towne strain has been  
100 used for vaccine development. [4]

101

102 The TB40/E strain was created by transfecting human foreskin fibroblast cells (HFF)

103 transfected by a TB40-BAC4 clone and propagated by standard procedures as  
104 described in detail [2]. The viral titers were designated by the 50% tissue culture  
105 infection dose (TCID<sub>50</sub>) method using human foreskin fibroblast cells infected with  
106 serially diluted supernatants.

107

### 108 **Real-time RT-PCR**

109 Total RNA was isolated from HTMC<sub>2</sub> at the indicated time points after infection by  
110 the two HCMV strains and reverse transcribed using the QuantiTect Reverse  
111 Transcription Kit (Qiagen). The cDNAs were amplified and quantified by the  
112 LightCycler (Roche, Mannheim, Germany) using the QuantiTect SYBR Green PCR  
113 kit. The sequences of the real-time PCR primer pairs were:

114 **IE-1:**

115 forward 5'- CCTCCAAGGTGCCACGGCCCGA-3',

116 reverse 5'- CATCCTCCCATCATATTA-3'.

117 **UL83 (pp65):**

118 forward 5'- GTCAGCGTTCGTGTTTCCCA-3',

119 reverse 5'- GGGACACAACACCGTAAAGC-3'.

120 **Glycoprotein B (gB):**

121 forward 5'- GGGACACAACACCGTAAAGC-3',



122 reverse 5'- ATGATGCCCTCRTCCARGTC-3'.

123 Interferon- $\beta$  (IFN- $\beta$ ):

124 forward 5'-CATTACCTGAAGGCCAAGGA -3',

125 reverse 5'-CAATTGTCCAGTCCCAGAGG-3'

126 Myosin phosphatase Rho interacting protein (MPRIP):

127 forward 5'- CTCTCCACACACGAGCTGAC-3',

128 reverse 5'- TCTTCTGGTGCGTTTCTTCC-3'

129

130 Monocyte chemotactic protein-1 (MCP-1):

131 forward 5'- AGGTGACTGGGGCATTGAT-3',

132 reverse 5'- GCCTCCAGCATGAAAGTCTC-3'

133

134 Glyceraldehyde-3-phosphate dehydrogenase (GAPDH):

135 forward 5'- AGCCACATCGCTCAGACAC-3',

136 reverse 5'- GCCCAATACGACCAAATCC-3'.

137

138 To measure the degree of viral DNA replication, HTMC<sub>5</sub> were infected with either the

139 TB40/E or the Towne strain, and viral DNA was extracted from the cells at the

140 indicated time points with the QiaAmp DNA mini kit (Qiagen, Hilden, Germany). The

141 extracted DNA was amplified with the LightCycler (Roche, Base, Switzerland) and  
142 normalized to known dilutions of synthesized pp65 DNA fragments.

143

#### 144 **Western blot**

145 HTMC<sub>s</sub> were infected with the TB40/E strain or the Towne strain at a selected  
146 multiplicity of infection (MOI). Cell lysates were harvested at 1, 2, and 3 days post  
147 infection (PI), and 10 µg of protein/lane were electrophoresed. The transferred  
148 membrane were stained with antibodies for HCMV IE1( NEA-9221, Perkin Elmer,  
149 Boston, MA), pp65 (CA003, EastCoast Bio, North Berwick, Maine, USA), or UL44  
150 (CH167, Santa Cruz, Santa Cruz, CA) [5]. The proteins were made visible with  
151 horseradish peroxidase-conjugated secondary antibody and chemiluminescence  
152 substrate as described [2].

153

#### 154 **Immunocytochemistry**

155 HTMC<sub>s</sub> were infected with HCMV at MOI of 5 and stained for HCMV proteins with  
156 mouse anti-HCMV monoclonal antibody against IE-1 (MAB8129, Millipore,  
157 Darmstadt, Germany) or pp65 (ab31624, Abcam, Cambridge, UK), or glycoprotein B  
158 (gB; ab6499, Abcam, Cambridge, UK). IE1, pp65, and gB were made visible by  
159 incubation with Alexa 488 conjugated-secondary antibody and stained for actin

160 cytoskeleton using phalloidin. Images were photographed with a confocal  
161 microscope (LSM710, Zeiss, Germany).

162

### 163 **Electron microscopy (EM)**

164 HTMC<sub>s</sub> were infected with either the TB40/E strain or the Towne strain of HCMV and  
165 fixed with 2.5% glutaraldehyde in 0.1 M sodium cacodylate buffer. After post fixation  
166 with 1% OsO<sub>4</sub> in 0.1 M sodium cacodylate buffer, cells were stained with 1% uranyl  
167 acetate. Cells were dehydrated, embedded in Epon 812, and sectioned with a  
168 microtome. The sections were stained with 4% uranyl acetate and 0.4% lead citrate  
169 and were examined by transmission electron microscopy (TEM).

170

### 171 **Statistical analyses**

172 Data are presented as the means  $\pm$  standard error of the means (SEMs). Statistical  
173 analyses were performed by *t* test, Mann Whitney U test, or ANOVA with post hoc  
174 test.

175

### 176 **Results**

177 When HTMCs were infected with the Towne strain of HCMV at an MOI of 5, an  
178 induction of the viral immediate early protein, 1E1, was detected at 6 h, and there

179 was a gradual increase to 24 h post infection (Fig. 1a right). The transcriptions of the  
180 delayed early proteins, gB, and leaky late protein, pp65, were also increased at 24 h  
181 PI (Fig.1b, 1c, right).

182

183 When HTMCs were infected with the TB40/E strain, IE1 was induced at 6 h. The  
184 induction kinetics of gB and pp65 were similar to that following the standard  
185 laboratory Towne strain infection, however the induction levels were significantly  
186 higher (Fig. 1).

187

188 HCMV-infected HTMCs were examined for IE1, pp65, and DNA polymerase  
189 processivity subunit UL44 by western blot analysis (Fig. 2). Consistent with the gene  
190 transcription outcomes, the IE1 protein was promptly induced at 1-day PI with both  
191 strains. Notably, TB40/E induced the expression of pp65 as early as 1-day PI at low  
192 MOI. In contrast, Towne infection required 3 days at high MOI for the induction. With  
193 TB40/E infection, the UL44 induction was also earlier at 2 days PI compared to 3  
194 days PI with the Towne strain.

195

196 We next determined whether HCMV infection will induce the antiviral responses of  
197 the host cells, regulation of cytoskeleton, and MCP-1 as an IOP-related cytokine.

198 [14] When HTMCs were infected with the TB40/E strain, there was a significant  
199 induction of interferon- $\beta$  (Fig. 3). In contrast, infection by the Towne strain did not  
200 induce interferon- $\beta$ .

201

202 We then examined whether HCMV infection will induce the regulatory factors for  
203 actin cytoskeleton (Fig. 4). After infection by the TB40/E strain of HCMV, the  
204 induction of the myosin phosphatase Rho interacting protein (MPRIIP) was  
205 significantly increased in the HTMCs. Again, Towne infection did not induce MPRIIP  
206 appreciably. Both strains induced MCP-1 in response to HCMV infection, however a  
207 prolonged induction was observed after TB40/E infection at 24 h PI (Fig. 5).

208

209 The location of the viral protein expression and actin stress fiber formation after  
210 HCMV infection was determined by immunostaining (Fig. 6). Intense IE1 staining  
211 of the nuclei of HTMCs was detected at 2 day PI with nuclear F-actin [6]. The  
212 expression of IE1 moved to the assembly compartment in the cytoplasm at 3 days  
213 PI. (Fig. 6a, 6b; upper panel) The expression of pp65 was also detected in the nuclei  
214 at 2 days PI (Fig 6c.), and it was localized to the viral assembly compartments in the  
215 cytoplasm at 3 days PI. (Fig. 6a, 6b; lower panel) The expression of gB was delayed  
216 and its expression was observed at 3 days PI. (Fig. 6a, 6b; middle panel)

217

218 When HTMCs were infected by TB40/E, an owl's eye appearance was observed in  
219 the nucleus with IE staining earlier than after Towne infection (Fig. 6a; white arrow),  
220 and it was detected as early as 1-day PI. (Fig. 6a; upper left) The level of expression  
221 increased in the cytoplasm at 3 days PI.

222

223 The expressions of pp65 and gB were observed in the nuclei at 2 days PI, and they  
224 were also localized in the viral assembly compartment and distinct stress fibers of  
225 actin were formed.

226

227 TB40/E infection induced significant remodeling of the actin cytoskeleton (Fig.  
228 6c) Thus, the TB40/E infection was more robust with an earlier expression of viral  
229 proteins and actin stress fiber formation.

230

231 The replication of viral DNA in HTMCs was assessed after infection with the TB40/E  
232 strain or the Towne strain (Fig. 7). Both strains induced significant increases of viral  
233 genome at 2 days PI at MOI of 5, and the increase continued, and both strains  
234 supported an efficient replication at MOI 1. Interestingly, TB40/E infection induced 5  
235 times more viral replication than the Towne strain at day 3 PI.

236

237 HCMV infected HTMC were examined by TEM. Infection by either the TB40/E strain  
238 or the Towne strain led to many viral particles and electron-dense particles (dense  
239 bodies) in the cytoplasm of the HTMCs (Fig. 8).

240

241 Then, we compared the increase in the level of the TB40/E and Towne strains in  
242 HTMC using titration by TCID<sub>50</sub>. HTMCs were infected with TB40/E or Towne at MOI  
243 of 1 and 5, and titrated (Fig. 9). TB40/E led to a continuous increase until day 11 PI  
244 and reached 10<sup>7</sup> TCID<sub>50</sub>. In contrast, the increase of the Towne strain reached a  
245 plateau at day 5 PI, and the maximum viral titer remained 10 times lower than that of  
246 TB40/E.

247

## 248 **Discussion**

249 Earlier studies have shown that infection of the anterior segment of the eye by  
250 HCMV can cause endotheliitis or iritis. Both diseases are characterized by an  
251 elevation of the IOP which is not observed for HCMV retinitis. Thus, anterior segment  
252 infections by HCMV may belong to a unified spectrum of a disease. Under these  
253 conditions, an IOP elevation can be caused by an increase in the outflow resistance  
254 in which the trabecular meshwork cells play a major role.

255

256 Steroid treatment is well known to induce steroid-induced glaucoma and impair the  
257 outflow function of the trabecular meshwork. When the trabecular meshwork cells  
258 were exposed to dexamethasone in vitro, there is a remodeling of the actin fibers  
259 and an induction of contraction [7]. Thus, stress fiber formation and actin remodeling  
260 were suggested as possible mechanisms of the secondary glaucoma. Our results  
261 showed that HCMV can replicate in HTMCs and reorganize the actin cytoskeleton of  
262 the cells [2]. This may explain why there was an elevation of the IOP associated with  
263 HCMV infection.

264

265 In eyes with open angle glaucoma, IL-4, IL-6, IL-8, IL-16, CCL2(MCP-1), TGF-β1,  
266 CCL13, CCL15, CCL22, CCL24, CXCL13, CXCL16, and TNF-α were found to be  
267 significantly elevated in the aqueous humor. [8]-[13]. Of these, the elevation of MCP-  
268 1 is consistent, and MCP-1 is a representative cytokine whose level is significantly  
269 correlated with the elevation of the IOP. [14] MCP-1 is well known to attract  
270 mononuclear cells and also induce collagen synthesis by TGF-β1 induction [15]. It  
271 also induces the production of matrix metalloproteinase-1 and tissue inhibitor of  
272 metalloproteinase-1 (TIMP-1). All of these changes may explain the induction of  
273 fibrotic change of outflow system leading to the IOP elevation.



274

275 Very recently, the AD169 strain of HCMV was reported to be able to infect  
276 HTMCs. [16] AD169 infection induced TGF $\beta$ 1 but its induction required at least 3  
277 days, and the induction levels remained within 10-20% of that of mock infection.  
278 Moreover, AD169 infection did not induce any mRNA of cytoskeleton-related  
279 molecules including fibronectin,  $\alpha$ -SMA, and collagen type 1A. This suggests less  
280 fibrogenic ability of AD169 which is in marked contrast to dexamethasone treatment  
281 to HTMCs, which induced fibronectin and  $\alpha$ -SMA.

282

283 We have shown that HCMV can proliferate in primary corneal endothelial cells, and  
284 TB40/E is tropic for corneal endothelium as well as vascular endothelium [2]. This\_  
285 led us to hypothesize that endotheliotropic strains can cause more relevant disease  
286 characteristics. The results showed that the endothelial cell tropic TB40/E proliferate  
287 very efficiently in trabecular meshwork cells with marked actin cytoskeleton stress  
288 fiber formation. This implicates the endothelial type of HCMV infection to be the  
289 cause of the higher virulence.

290

291 In HCMV endotheliitis, the copy numbers of the DNA of HCMV in the aqueous humor  
292 determines the frequency of recurrences, degree of IOP elevation, and endothelial

293 cell loss [17]. These findings indicate that the copy number of the viral genome  
294 determines the course of the disease and refractoriness. The adaptive Towne strain  
295 also proliferated in HTMCs, however the TCID<sub>50</sub> remained 10 times lower than that  
296 of TB40/E for HTMCs and corneal endothelial infections. The TB40/E strain  
297 proliferated well in corneal endothelial cells and required 4 days to reach a plateau  
298 with high tissue culture infective dose (TCID) titers. Thus, the trabecular meshwork  
299 cells supported both the endotheliotropic and adaptive strains however the TB40/E  
300 strain was more efficient in proliferation and had a higher virulence in HTMCs.

301

302 Contraction and reorganization of the actin stress fibers presumably play important  
303 roles in the IOP regulation through the conventional outflow channels. Rho kinase  
304 inhibitors reorganize or disrupt F-actin fibers through Rho GTPase proteins, and they  
305 were recently made available for use on patients to reduce the IOP by targeting the  
306 outflow through Schlemm's canal. HCMV diverts the actin fiber transport system of  
307 the host to organize nuclear egress, viral assembly, and egress from the cytoplasm.  
308 Thus, HCMV infection disrupts or reorganizes the actin fiber cytoskeleton. For  
309 example, US-28 protein of HCMV activates the RhoA-mediated motility and the  
310 ROCK pathway [18, 19]. In the intracellular viral assembly complex of the host, RhoB  
311 is diverted to reorganize or disrupt actin stress fibers leading to efficient viral

312 production [20].

313

314 Adaptive HCMV strains, including the Towne and AD169 strains, proliferate well in  
315 fibroblasts, however macrophages, dendritic cells, vascular endothelial cells, and  
316 epithelial cell do not allow efficient proliferation. These strains are deficient by as  
317 many as 20 genes [21], including pUL128, pUL130, and ppUL131A, which mediate  
318 viral entry into endothelial cells or epithelial cell lineage [22, 23]. However, whether  
319 these factors and other viral genes determine the pathogenicity of HCMV has not  
320 been determined.

321

322 We observed the induction of IE1 transcript and gene products in the HTMCs. The  
323 induction of IE1 determines the latency or reactivation of HCMV in the infected cells.

324 A strong induction of IE1 by the TB40/E strain indicates a facilitated activation of viral  
325 gene induction (Figure 1, 2). However, IE1 expression is not a reliable marker of viral  
326 infection because it can be induced without viral replication. IE1 is induced even in  
327 non-permissive animal cells because of its very potent promotor activity.

328

329 We showed a strong induction of the pp65 protein which strongly inhibits antiviral  
330 interferon responses, and it can serve as the major target of the host acquired

331 immune system. The HCMV proteins, including pp65, provoke strong acquired  
332 immunity of CD8<sup>+</sup> T cells through MHC class I recognition pathway. Because of the  
333 high prevalence of HCMV infection in elderly subject, [24] up to 30% of CD8<sup>+</sup> T cells  
334 in their bodies responsive to HCMV antigen [25]. This substantial expansion of CD8<sup>+</sup>  
335 T cells that are memory inflated is often facilitated by antigen presentation by non-  
336 hematopoietic cells including endothelial cells [26, 3]. This immunostimulatory effect  
337 of infected cells is characterized by potent interferon responses which we showed for  
338 TB40/E infection.

339

340 gB mediates the adhesion of HCMV to the host heparan sulfate proteoglycan. Thus,  
341 neutralization of gB by antibody generation is an important strategy of the host to  
342 prevent cell-to-cell spread or cell fusion after infection. Collectively, the strong  
343 expression of pp65 and gB by the trabecular meshwork cells and the reactivity of the  
344 host acquired immunity may determine the clinical characteristics of the disease.

345

346 There are some limitations for our study. Our analysis was based on an in vitro  
347 infection model of cultured trabecular meshwork cells. This may not reflect the in vivo  
348 role of trabecular meshwork including the conventional outflow of aqueous humor. In  
349 addition, the inflammatory cells recruited by CMV-induced inflammation in vivo, may

350 cause remodeling of trabecular meshwork. However, our finding that the  
351 endotheliotropic strain of HCMV is pathogenic in both the corneal endothelium and  
352 trabecular meshwork is important information to understand the disease etiology.

353

354 In conclusion, HCMV can infect trabecular meshwork cells and promote the  
355 reorganization of the actin cytoskeleton. This then presumably leads to the IOP  
356 elevation in the host. Understanding the viral and host aspects of HCMV infection  
357 may provide important clues to develop efficacious treatment of refractory anterior  
358 segment infection by HCMV.

359 **Acknowledgments**

360 This work was supported by Grant-in-Aid 17K11481, 17K16969, and 16K11322 for  
361 Scientific Research from the Japanese Ministry of Education, Science, and Culture.  
362

363 **References**

364

365 1. Koizumi N, Inatomi T, Suzuki T, Shiraishi A, Ohashi Y, Kandori M et al. Clinical features and  
366 management of cytomegalovirus corneal endotheliitis:analysis of 106 cases from the Japan corneal  
367 endotheliitis study. Br J Ophthalmol. 2014:in press.

368 2. Hosogai M, Shima N, Nakatani Y, Inoue T, Iso T, Yokoo H et al. Analysis of human cytomegalovirus  
369 replication in primary cultured human corneal endothelial cells. Br J Ophthalmol. 2015;99:1583-90.  
370 doi:10.1136/bjophthalmol-2014-306486.

371 3. Miyazaki D, Uotani R, Inoue M, Haruki T, Shimizu Y, Yakura K et al. Corneal endothelial cells activate  
372 innate and acquired arm of anti-viral responses after cytomegalovirus infection. Exp Eye Res.  
373 2017;161:143-52. doi:10.1016/j.exer.2017.06.017.

374 4. Bradley AJ, Lurain NS, Ghazal P, Trivedi U, Cunningham C, Baluchova K et al. High-throughput  
375 sequence analysis of variants of human cytomegalovirus strains Towne and AD169. J Gen Virol.  
376 2009;90:2375-80. doi:10.1099/vir.0.013250-0.

377 5. Isomura H, Stinski MF, Murata T, Yamashita Y, Kanda T, Toyokuni S et al. The human cytomegalovirus  
378 gene products essential for late viral gene expression assemble into prereplication complexes before  
379 viral DNA replication. J Virol. 2011;85:6629-44. doi:10.1128/JVI.00384-11.

380 6. Wilkie AR, Lawler JL, Coen DM. A Role for Nuclear F-Actin Induction in Human Cytomegalovirus  
381 Nuclear Egress. MBio. 2016;7. doi:10.1128/mBio.01254-16.

- 382 7. Clark AF, Wilson K, McCartney MD, Miggans ST, Kunkle M, Howe W. Glucocorticoid-induced  
383 formation of cross-linked actin networks in cultured human trabecular meshwork cells. *Invest*  
384 *Ophthalmol Vis Sci.* 1994;35:281-94.
- 385 8. Kuchtey J, Rezaei KA, Jaru-Ampornpan P, Sternberg P, Jr., Kuchtey RW. Multiplex cytokine analysis  
386 reveals elevated concentration of interleukin-8 in glaucomatous aqueous humor. *Invest Ophthalmol Vis*  
387 *Sci.* 2010;51:6441-7. doi:10.1167/iovs.10-5216.
- 388 9. Zenkel M, Lewczuk P, Jünemann A, Kruse FE, Naumann GOH, Schlötzer-Schrehardt U.  
389 Proinflammatory Cytokines Are Involved in the Initiation of the Abnormal Matrix Process in  
390 Pseudoexfoliation Syndrome/Glaucoma. *The American Journal of Pathology.* 2010;176:2868-79.  
391 doi:10.2353/ajpath.2010.090914.
- 392 10. Sawada H, Fukuchi T, Tanaka T, Abe H. Tumor necrosis factor-alpha concentrations in the aqueous  
393 humor of patients with glaucoma. *Invest Ophthalmol Vis Sci.* 2010;51:903-6. doi:10.1167/iovs.09-4247.
- 394 11. Ghanem A, Arafa L, Elewa A. Tumor Necrosis Factor- $\alpha$  and Interleukin-6 Levels in patients with  
395 primary open-angle Glaucoma. *J Clin Exp Ophthalmol.* 2011;2:2.
- 396 12. Chua J, Vania M, Cheung CMG, Ang M, Chee SP, Yang H et al. Expression profile of inflammatory  
397 cytokines in aqueous from glaucomatous eyes. *Molecular vision.* 2012;18:431.
- 398 13. Garweg JG, Zandi S, Pfister IB, Skowronska M, Gerhardt C. Comparison of cytokine profiles in the  
399 aqueous humor of eyes with pseudoexfoliation syndrome and glaucoma. *PloS one.* 2017;12:e0182571.
- 400 14. Kokubun T, Tsuda S, Kunikata H, Yasuda M, Himori N, Kunimatsu-Sanuki S et al. Characteristic



401 Profiles of Inflammatory Cytokines in the Aqueous Humor of Glaucomatous Eyes. *Ocular Immunology*  
402 *and Inflammation*. 2017;1-12.

403 15. Yamamoto T, Eckes B, Mauch C, Hartmann K, Krieg T. Monocyte chemoattractant protein-1  
404 enhances gene expression and synthesis of matrix metalloproteinase-1 in human fibroblasts by an  
405 autocrine IL-1 $\alpha$  loop. *The Journal of Immunology*. 2000;164:6174-9.

406 16. Choi JA, Kim JE, Noh SJ, Kyoung Kim E, Park CK, Paik SY. Enhanced cytomegalovirus infection  
407 in human trabecular meshwork cells and its implication in glaucoma pathogenesis. *Sci Rep*.  
408 2017;7:43349. doi:10.1038/srep43349.

409 17. Kandori M, Miyazaki D, Yakura K, Komatsu N, Touge C, Ishikura R et al. Relationship between the  
410 number of cytomegalovirus in anterior chamber and severity of anterior segment inflammation. *Jpn J*  
411 *Ophthalmol*. 2013;57:497-502. doi:10.1007/s10384-013-0268-2.

412 18. Vomaske J, Varnum S, Melnychuk R, Smith P, Pasa-Tolic L, Shutthanandan JI et al. HCMV pUS28  
413 initiates pro-migratory signaling via activation of Pyk2 kinase. *Herpesviridae*. 2010;1:2.  
414 doi:10.1186/2042-4280-1-2.

415 19. Langemeijer EV, Slinger E, de Munnik S, Schreiber A, Maussang D, Vischer H et al. Constitutive  
416 beta-catenin signaling by the viral chemokine receptor US28. *PLoS One*. 2012;7:e48935.  
417 doi:10.1371/journal.pone.0048935.

418 20. Goulidaki N, Alarifi S, Alkahtani SH, Al-Qahtani A, Spandidos DA, Stournaras C et al. RhoB is a  
419 component of the human cytomegalovirus assembly complex and is required for efficient viral

420 production. *Cell Cycle*. 2015;14:2748-63. doi:10.1080/15384101.2015.1066535.

421 21. Cha TA, Tom E, Kemble GW, Duke GM, Mocarski ES, Spaete RR. Human cytomegalovirus clinical  
422 isolates carry at least 19 genes not found in laboratory strains. *J Virol*. 1996;70:78-83.

423 22. Revello MG, Gerna G. Human cytomegalovirus tropism for endothelial/epithelial cells: scientific  
424 background and clinical implications. *Reviews in medical virology*. 2010;20:136-55.  
425 doi:10.1002/rmv.645.

426 23. Ryckman BJ, Chase MC, Johnson DC. HCMV gH/gL/UL128-131 interferes with virus entry into  
427 epithelial cells: evidence for cell type-specific receptors. *Proc Natl Acad Sci U S A*. 2008;105:14118-23.  
428 doi:10.1073/pnas.0804365105.

429 24. Moorman NJ, Cristea IM, Terhune SS, Rout MP, Chait BT, Shenk T. Human cytomegalovirus protein  
430 UL38 inhibits host cell stress responses by antagonizing the tuberous sclerosis protein complex. *Cell*  
431 *Host Microbe*. 2008;3:253-62. doi:10.1016/j.chom.2008.03.002.

432 25. Sylwester AW, Mitchell BL, Edgar JB, Taormina C, Pelte C, Ruchti F et al. Broadly targeted human  
433 cytomegalovirus-specific CD4+ and CD8+ T cells dominate the memory compartments of exposed  
434 subjects. *J Exp Med*. 2005;202:673-85. doi:10.1084/jem.20050882.

435 26. Klenerman P, Oxenius A. T cell responses to cytomegalovirus. *Nat Rev Immunol*. 2016;16:367-77.  
436 doi:10.1038/nri.2016.38.

437

438 **Figure legends**

439 **Figure 1. Induction of the mRNA of the genes of human cytomegalovirus**  
440 **(HCMV) in human trabecular meshwork cells (HTMC) after HCMV infection**

441 HTMCs were infected with the Towne strain or the TB40/E strain of HCMV, and the  
442 induction of the mRNA of IE1(a), pp65 (b), and glycoprotein B (gB)(c) was  
443 determined by RT-real-time PCR. Viral genes, IE1, pp65, and gB, were sequentially  
444 induced after infection by the Towne strain or the TB40/E strain of HCMV. TB40/E  
445 induced significantly higher amounts of IE1, pp65, and gB.

446 \*:  $P = 0.05$ , \*\*:  $P = 0.05$ ;  $n = 8$

447

448 **Figure 2. Induction kinetics of viral gene proteins in HTMCs after HCMV**  
449 **infection.**

450 HTMCs were infected with the Towne strain or the TB40/E strain at MOI of 1 or 5,  
451 and the extracted viral proteins were assayed by western blot analyses. The proteins  
452 of IE1, pp65, and UL44 were sequentially expressed after the HCMV infection.  
453 Infection by the TB40/E strain led to stronger inductions of pp65 and UL44.

454

455 **Figure 3. Induction of interferon response in HTMCs after infection by the**  
456 **TB40/E strain of HCMV.**

457 The extracted mRNA at 6 h post infection was evaluated for interferon using real-  
458 time RT-PCR for interferon- $\beta$ . TB40/E infection induced significantly higher levels of  
459 interferon- $\beta$  than Towne. \*:  $P = 0.016$ , \*\*:  $P = 0.0001$ ;  $n = 5$ .

460

461 **Figure 4. Induction of myosin phosphatase Rho interacting protein (MPRIP) in**  
462 **HTMCs after infection by the TB40/E strain of HCMV.**

463 HTMCs were infected with the TB40/E strain or the Towne strain. The level of mRNA  
464 induction of myosin phosphatase Rho interacting protein (MPRIP) was evaluated  
465 using RT-PCR. TB40/E infection induced significantly higher levels of MPRIP at 12 h  
466 PI than Towne. \* $P = 0.0001$ ;  $n = 5$ .

467

468 **Figure 5. Induction of MCP-1 in HTMCs after infection by HCMV**

469 HTMCs were infected with the TB40/E strain or the Towne strain. The level of mRNA  
470 induction of MCP-1 was evaluated using RT-PCR. TB40/E infection prolonged the  
471 induction of higher levels of MCP-1 at 24 h, while induction of MCP-1 by Towne was  
472 observed at 6 h PI and was transient. \*:  $P = 0.04$ , \*\*:  $P < 0.001$ ;  $n = 5$ .

473

474 **Figure 6. Induction of viral gene proteins and remodeling of actin**  
475 **cytoskeleton after HCMV infection.**

476 HTMCs were infected with the TB40/E strain (a) or the Towne strain (b) of HCMV at  
477 MOI of 5 and immunostained for IE1, pp65, and glycoprotein B (Green). TB40/E  
478 infection induced significant remodeling of the actin cytoskeleton (c, pp65,  
479 green). Actin was stained using phalloidin (red). Nucleus was labelled by DAPI  
480 (blue). \*: viral assembly compartment.

481

482 **Figure 7. Viral genome replication for HCMV in human trabecular meshwork**  
483 **cells (HTMCs).**

484 HTMCs were infected with the HCMV and examined for viral genomic copy  
485 equivalent using real-time PCR. Both the TB40/E strain and Towne strain induced  
486 significant increases of the viral genome. TB40/E infection induced 5 times more  
487 viral replication than Towne at day 3 post infection. n = 6

488

489 **Figure 8. Production of infectious virions after HCMV infection of human**  
490 **trabecular meshwork cells (HTMCs)**

491 HTMCs were infected with the TB40/E strain or the Towne strain of HCMV at MOI of  
492 0.1 and examined by electron microscopy. Viral particles (arrow) and dense bodies  
493 (arrowhead) can be seen in the cytoplasm. Bars indicate 500 nm (TB40/E) and 200  
494 nm (Towne).

495

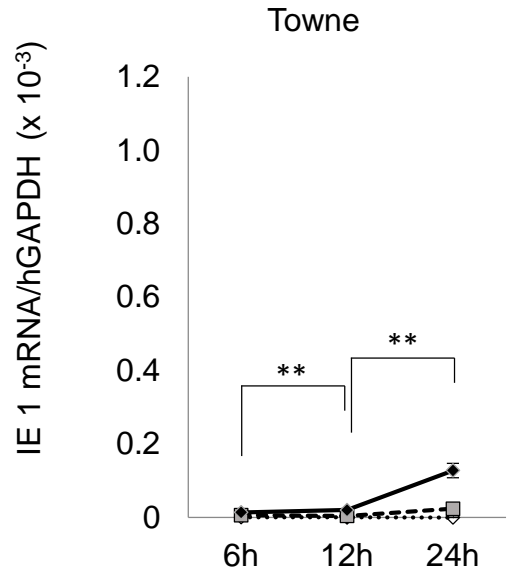
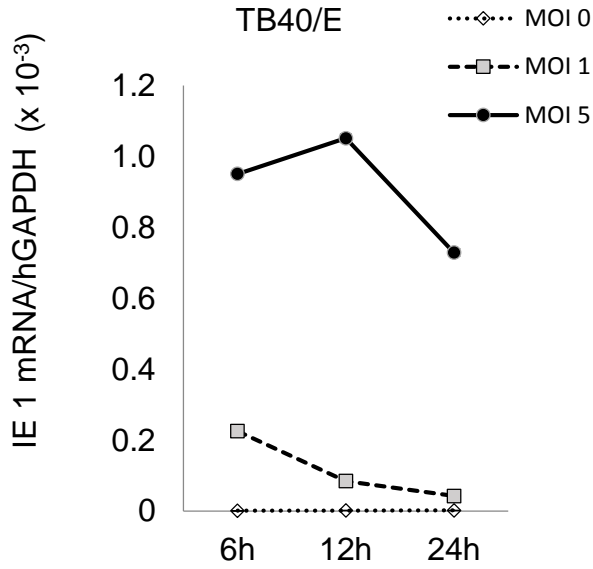
496 **Figure 9. Efficient growth of HCMV in HTMCs.**

497 HTMCs were infected with TB40/E or Towne at MOI of 1 and 5 and were titrated for  
498 tissue culture infectious dose (TCID<sub>50</sub>). Both strains had efficient growth in HTMCs.

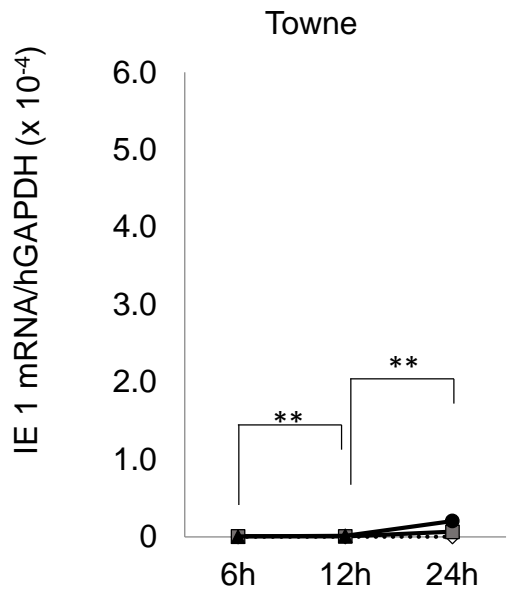
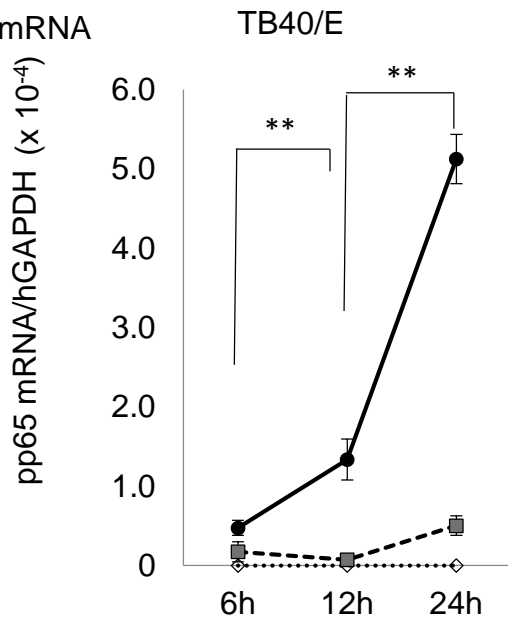
499 The maximum viral titer was significantly higher for the TB40/E strain. n = 4.

500

IE1 mRNA



pp65 mRNA



gB mRNA

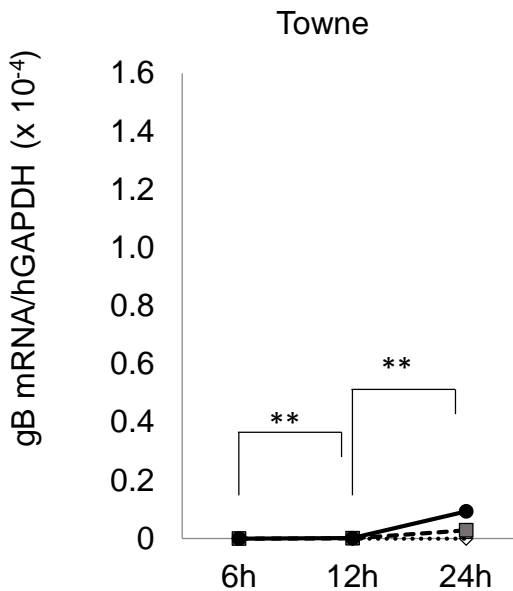
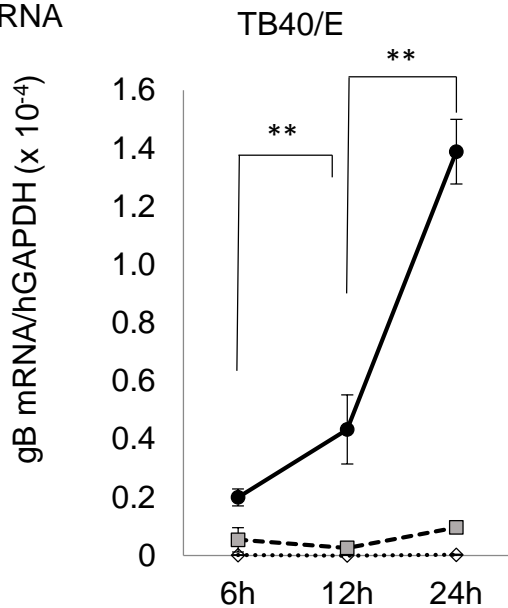


Figure.1

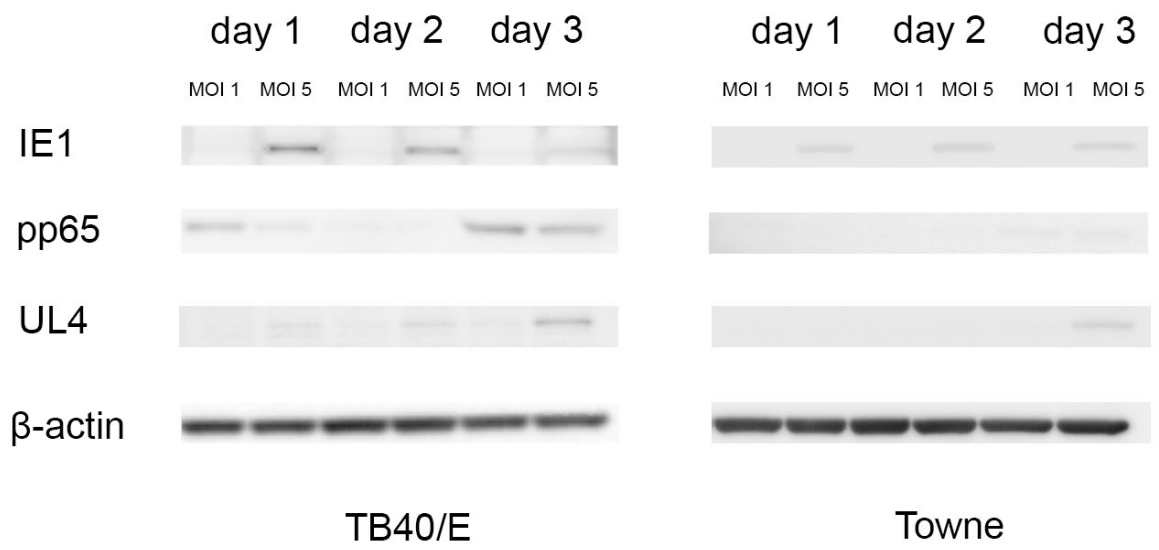


Figure.2



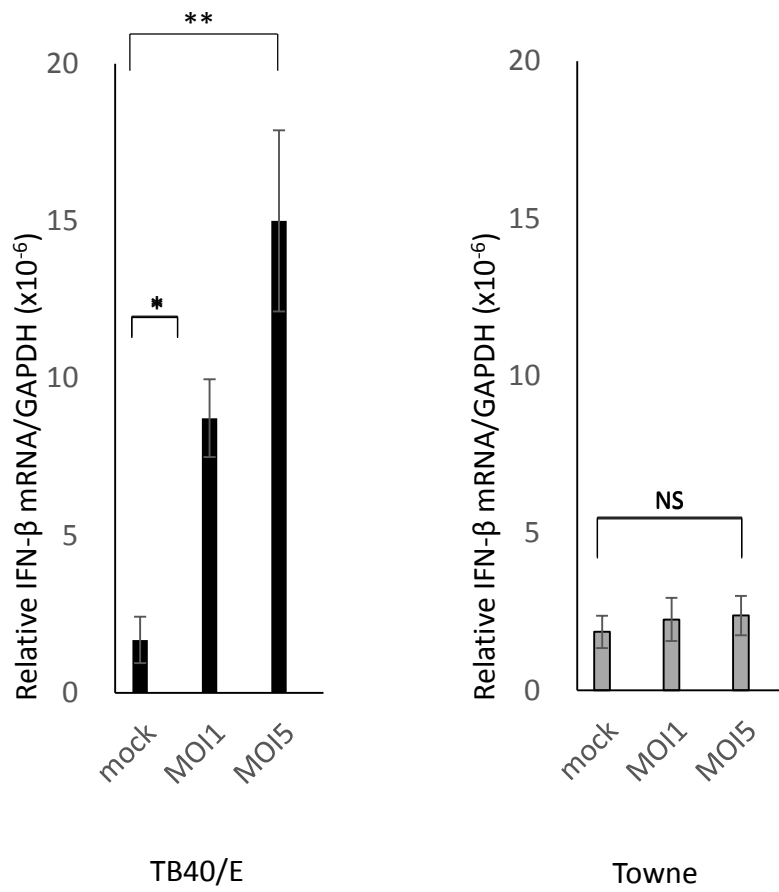


Figure.3

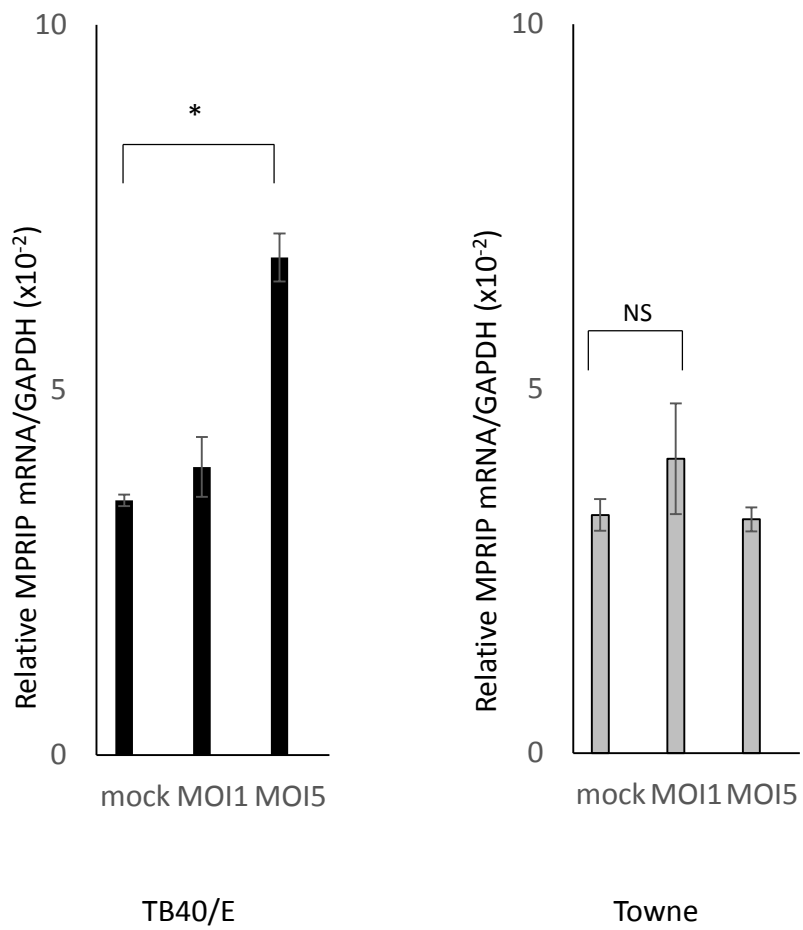


Figure.4

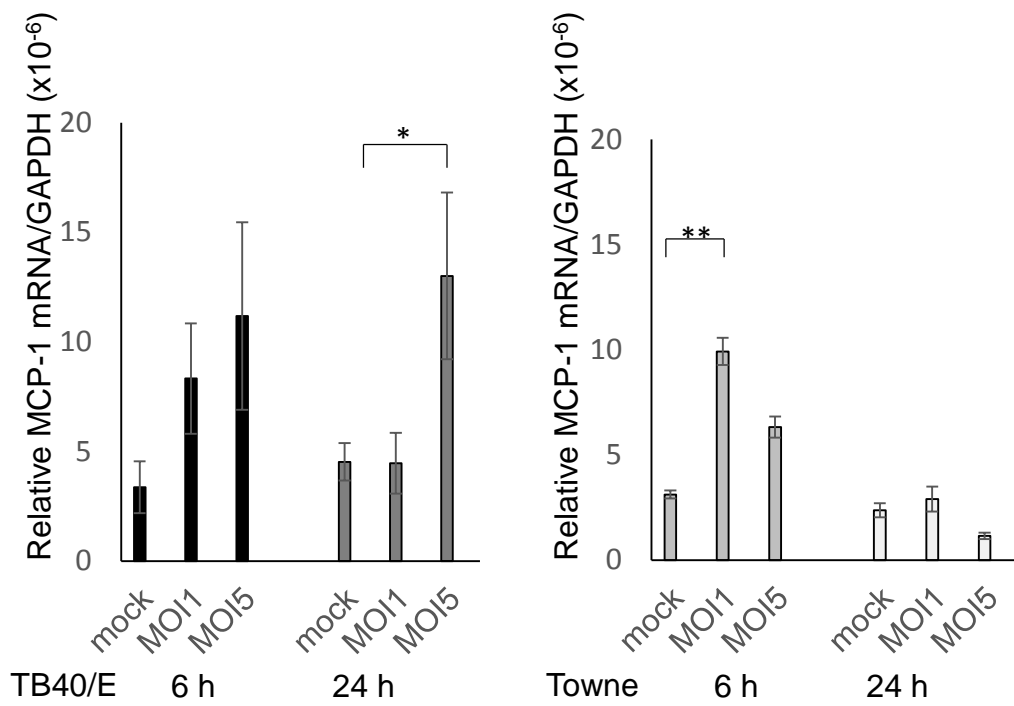
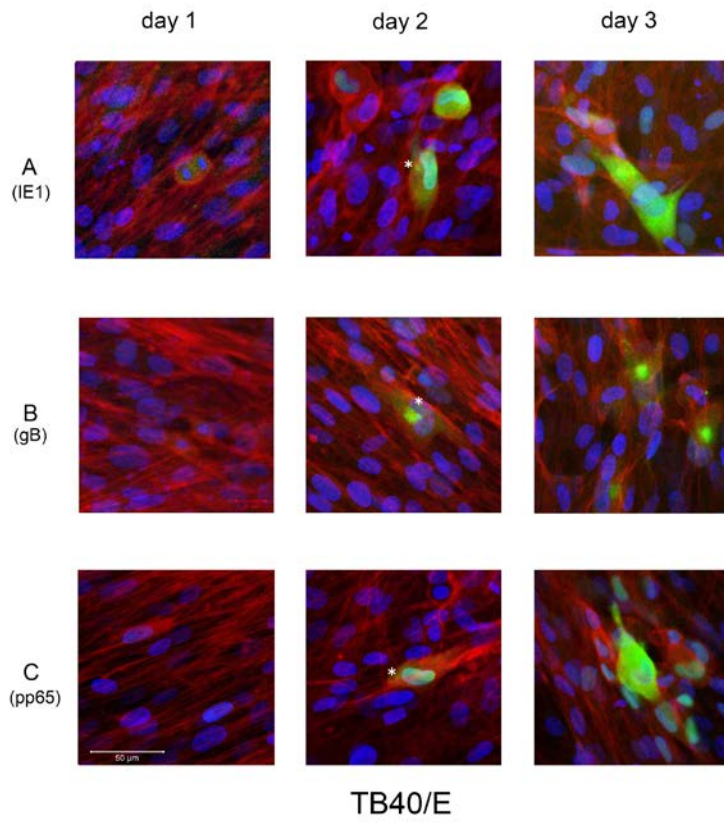
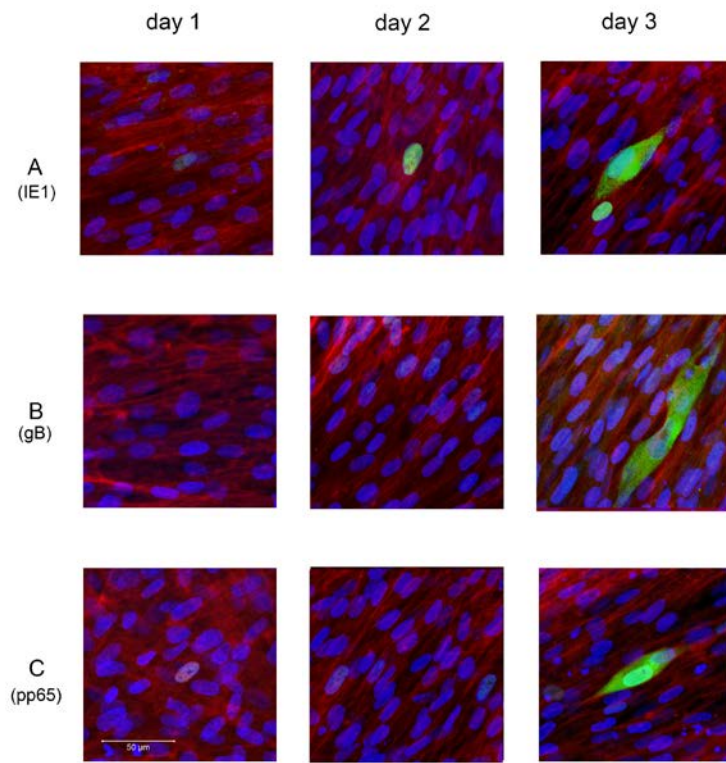


Figure.5



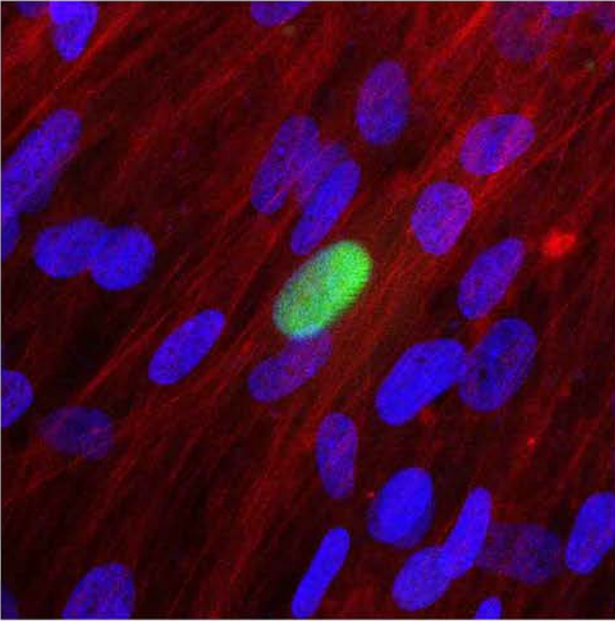
TB40/E



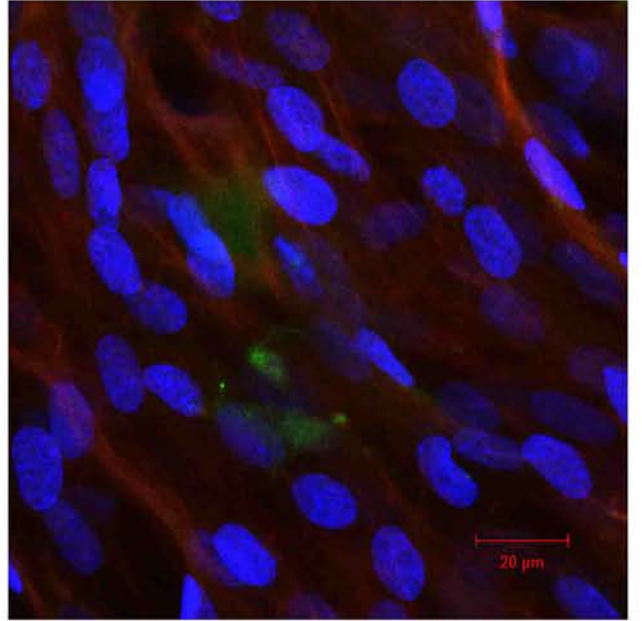
Towne

Figure.6

C.



TB40/E



Towne

Figure.6

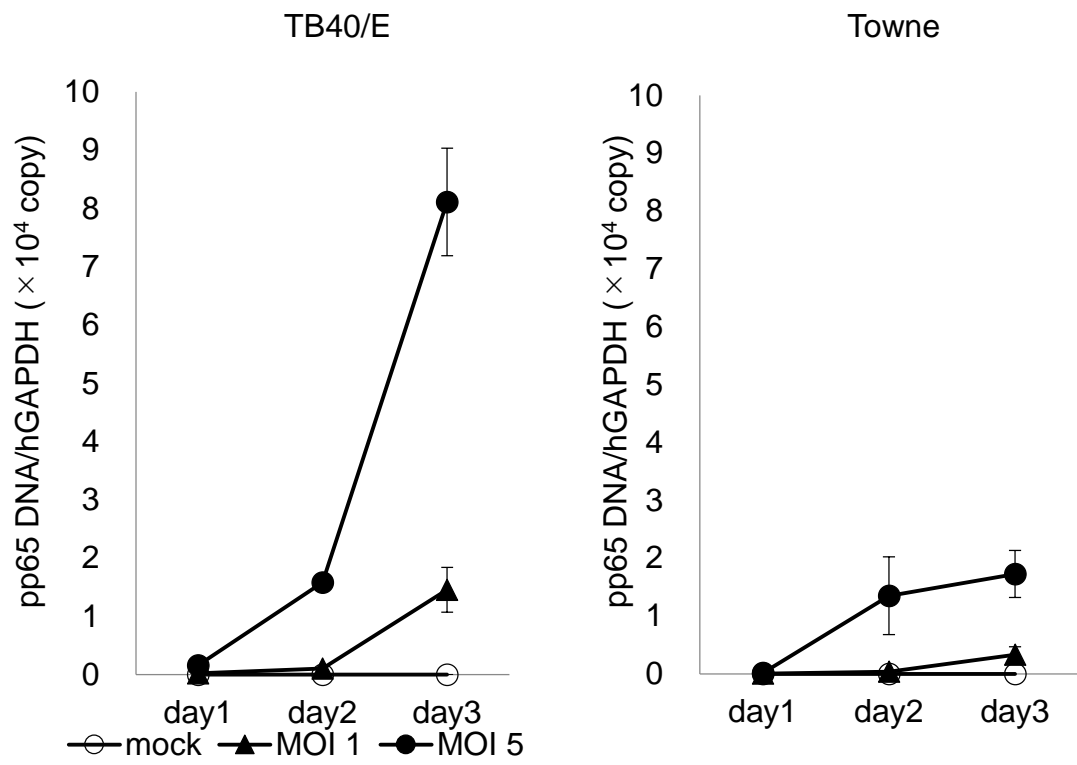
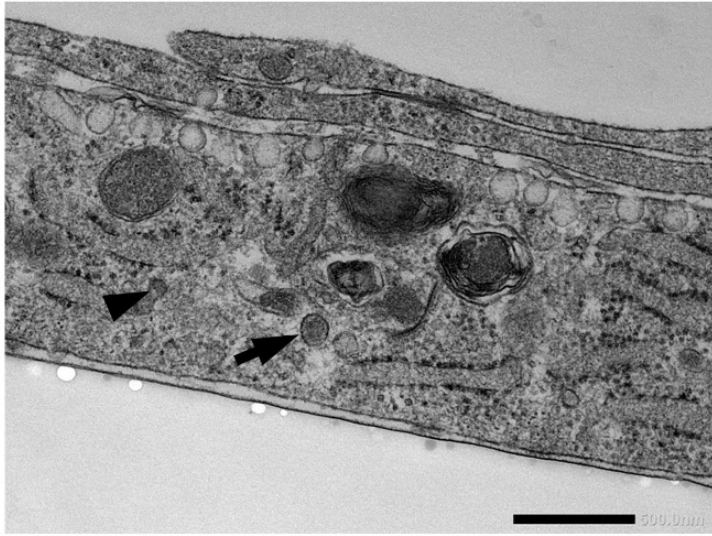
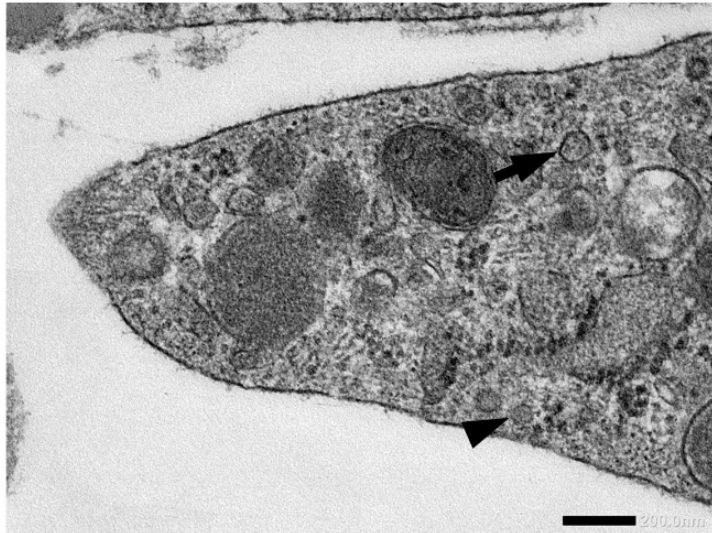


Figure.7



TB40/E



Towne

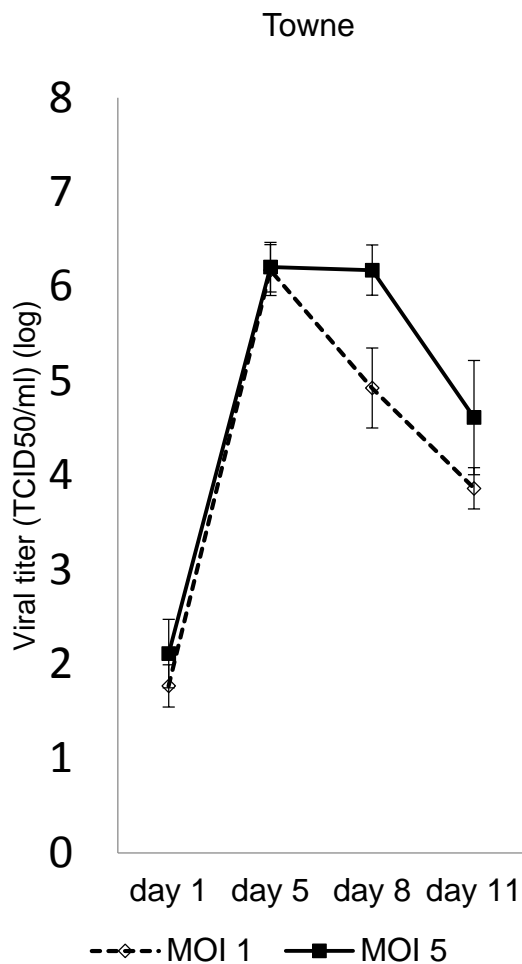
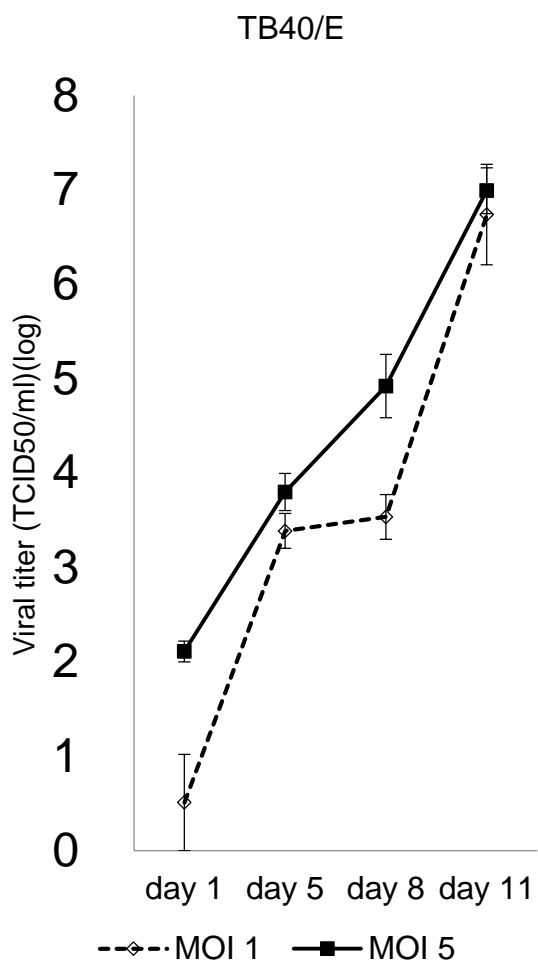


Figure.9